Zinc Metal Organic Frameworks: Efficient Catalysts for Diastereoselective Henry Reaction and Transesterification

Anirban Karmakar, M. Fátima C. Guedes da Silva and Armando J. L. Pombeiro*

Centro de Química Estrutural, Complexo I, Instituto Superior Técnico, Universidade de Lisboa, Av. Rovisco Pais, 1049–001 Lisbon, Portugal. E-mail: *pombeiro@tecnico.ulisboa.pt*

Abstract

Three new compounds bearing different flexible side functional groups, *viz.* 2-acetamidoterephthalic acid (H_2L1), 2-propionamidoterephthalic acid (H_2L2) and 2-benzamidoterephthalic acid (H_2L3), were synthesized and their coordination reactions with zinc(II) were studied. X-ray crystallography showed the formation of novel metal organic frameworks with different dimensionalities, where the side functional groups of amidoterephthalic acid and/or auxiliary ligands were found to play significant roles. These frameworks $[Zn_2(L1)_2(4,4'\text{-bipyridine})_2(H_2O)(DMF)]_n$ (**1**), $[Zn_4(L2)_3(OH)_2(DMF)_2(H_2O)_2]_n$ (**2**) and $[Zn(L3)(H_2O)_2]_n \cdot n/2(1,4\text{-dioxane})$ (**3**) act as heterogeneous polymeric solid catalysts not only for the diastereoselective nitroaldol (Henry) reaction of different aldehydes with nitroalkanes but also in transesterification reactions. These MOF-based heterogeneous catalysts can be recycled without losing activity.

Keywords: Carboxylate, Zinc, Metal Organic Frameworks, Crystal Structure analysis, X-ray diffraction, Catalysis.

Introduction

Porous metal–organic frameworks (MOFs), a combination of inorganic metal species and organic linkers, have attracted considerable attention in recent years[1]. MOFs can be readily prepared from the simple combination and self-assembly of metal ions with organic bridging ligands containing divergent donor atoms. This metal–ligand directed assembly approach can yield a new generation of multi-dimensional networks, which contain channels or cavities of various sizes and shapes[2]. Due to the porous features of such MOFs a wide range of applications can be envisioned namely in nonlinear optics[3], gas storage[4], catalysis[5] and host–guest induced separation[6]. Catalytic applications of such materials were among the earliest proposed ones[7], and nowadays many organic reactions can be efficiently catalyzed by MOFs[8].

A remarkable advancement has been achieved in recent years in the development of porous MOFs by using multidentate aromatic carboxylate ligands, due to their robustness and thermal stability.[9-10] Some earlier reports relate to the use of dicarboxylate [11-12], tricarboxylate[13-15] and tetracarboxylate[16-21] linkers that are inter-bridged by mono- or multi-nuclear metal nodes, leading to stable MOFs with permanent porosity[22]. MOFs can work as catalysts through two different components[23] *viz.* the metal ions, which

either provide the coordinatively unsaturated nodes and/or form the active metal sites integrated into the linker ligand, and the coordinated ligands. Hence, depending on the nature of the ligands and binding metal ions MOFs can act as Lewis bases or acids in the catalytic medium.

The Henry or nitroaldol reaction is known as one of the most powerful and atom-economic reactions for C–C bond formations with various functionalized structural motifs.[24-25] Usually this reaction is performed with homogeneous basic catalysts, such as alkali metal hydroxides, alkoxides or amines, with a rather good efficiency.[26] Many homogeneous catalyst,[27-34] including some copper[34j, 34l] and zinc[34b, 34l] containing complexes obtained by our group, have already been reported. However, heterogeneous catalysts for such a transformation are rare.[35]

Transesterifications are important transformations in organic synthesis, in industrial and in academic laboratories[36], and have important applications in polyester synthesis and biodiesel production.[37] Homogenous catalysts have been reported to catalyze these reactions[38] but high reaction temperature and acidic conditions are usually required. Some other discrete complexes and coordination polymers can also catalyze such a type of reactions.[39] However, there is still a demand to develop new types of catalysts based on cheap and environmentally tolerable metal complexes, that could be easily recyclable (hence forming an heterogeneous system) and show a high efficiency under mild conditions.

Hence, we report herein the synthesis and characterization of new ligands bearing different amide side functional groups, 2-acetamidoterephthalic acid (H_2L1), 2-propionamidoterephthalic acid (H_2L2) and 2-benzamidoterephthalic acid (H_2L3) (Scheme 1), which were then applied to the synthesis, under hydrothermal conditions, of Zn(II)-frameworks. The structural features of the obtained Zn MOFs $[Zn_2(L1)_2(4,4'-bipyridine)_2(H_2O)(DMF)]_n$ (**1**), $[Zn_4(L2)_3(OH)_2(DMF)_2(H_2O)_2]_n$ (**2**) and $[Zn(L3)(H_2O)_2]_n$. $n/2(1,4-dioxane)$ (**3**), could be established by single crystal X-ray diffraction analysis and were subjected to a topological study.

The obtained frameworks act as heterogeneous catalysts in the nitroaldol combination of nitroethane with various aldehydes as well as in the transesterification reactions of various aromatic esters.
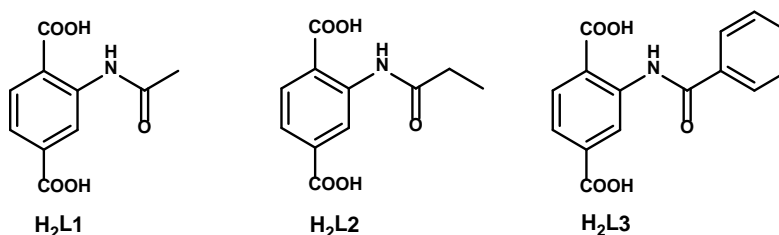
Scheme 1: Schematic representation of the H_2L1, H_2L2 and H_2L3 ligands

Results and Discussion

Syntheses and Characterization

The reaction of H_2L1, H_2L2 or H_2L3 with zinc(II) nitrate hexahydrate under hydrothermal reaction conditions leads to the formation of $[Zn_2(L1)_2(4,4'-bipyridine)_2(H_2O)(DMF)]_n$ (**1**), $[Zn_4(L2)_3(OH)_2(DMF)_2(H_2O)_2]_n$ (**2**) or $[Zn(L3)(H_2O)_2]_n$. $n/2(1,4-dioxane)$ (**3**), respectively [L1 = 2-

acetamidoterephthalate, L2 = 2-propionamidoterephthalate, L3 = 2-benzamidoterephthalate, DMF = dimethyl formamide].

In the IR spectra, the characteristic strong bands of coordinated carboxylate groups of **1**, **2** and **3** appear at 1564–1569 cm^{-1}or 1337-1372 cm^{-1} for the asymmetric or the symmetric stretching, respectively. The bands in the regions 1660–1610 cm^{-1} and 1417–1429 cm^{-1} are attributed to the C=C stretching frequency of the aromatic rings.[40] Due to their insolubility in common NMR solvents, these frameworks were only characterized by single crystal and powder X-ray diffraction, elemental and TG analysis.

Crystal structure analysis

In all the coordination polymers, the zinc metal ions are in the 2+ oxidation state and to fulfill the charge balance requirements the ligands are fully deprotonated.

The hydrothermal reaction of 2-acetamidoterephthalic acid (H$_2$L1) with zinc(II) nitrate hexahydrate in the presence of 4,4'-bipyridine lead to the formation of a 2D network [Zn$_2$(L1)$_2$(4,4'-bipyridine)$_2$(H$_2$O)(DMF)]$_n$ (**1**) extended with zinc(II), L1^{2-} ions and bipyridine molecules. Single-crystal X-ray diffraction studies reveal that **1** crystallizes in the monoclinic P2$_1$/c space group and that the asymmetric unit contains two zinc(II) ions whose coordination spheres are organized with two L1^{2-} ligands, two 4,4'-bipyridine molecules, one water molecule and one DMF molecule (Figure 1). This framework contains two identical networks which are interpenetrated forming a two dimensional structure with 2-fold interpenetrating networks (Figure 2).

The zinc(II) ions in **1** have two distinct coordination environments. Zn1 is in an octahedral coordination environment whose distortion can be assessed by the octahedral angle variance (OAV)[41a] and quadratic elongation (OQE) which assume values of 143 and 1.045, respectively. One of the carboxylate arms of two μ_2-L1^{2-} ligands bridges two Zn1 cations [Zn1–O8 and Zn1–O9] the coordination sphere of each metal being then fulfilled by ligating to every N-atoms of one of the bridging bipyridine molecules [Zn1–N5 and Zn1–N6] and to both oxygen atoms of a carboxylate group of the remaining L1^{2-} ligand [Zn1–O3 and Zn1–O4]. The Zn1 coordination mode constitutes a dinuclear core acting as a secondary building block unit in the construction of the two-dimensional polymeric assembly. The Zn2 cation is coordinated to one of the O-atoms of two distinct L1^{2-} ligands [Zn2–O1 and Zn2–O6] and further coordinated to the N-atom of a non-bridging bipyridine moiety [Zn2–N3], to a water molecule [Zn2–O12] and to a DMF residue [Zn2–O11], the latter two occupying the axial positions of a distorted trigonal bipyramidal coordination environment around the metal center (τ_5 = 0.82).[41b] Thus, in **1** the coordination behaviour of the two 4,4'-bipyridine molecules are different since one of them bridges between two Zn1 centers and the other is monodentateto Zn2; concerning the dicarboxylate ligands L1^{2-}, one occurs in non-bridging monodentate (μ_1-O, to Zn2) and *syn-anti*-type bridging bidentate (μ_2-O,O' to two Zn1) binding modes, while the other shows the μ_1-O type (to Zn2) as well as the chelating bidentate μ_1-O,O(to Zn1) ligating method.
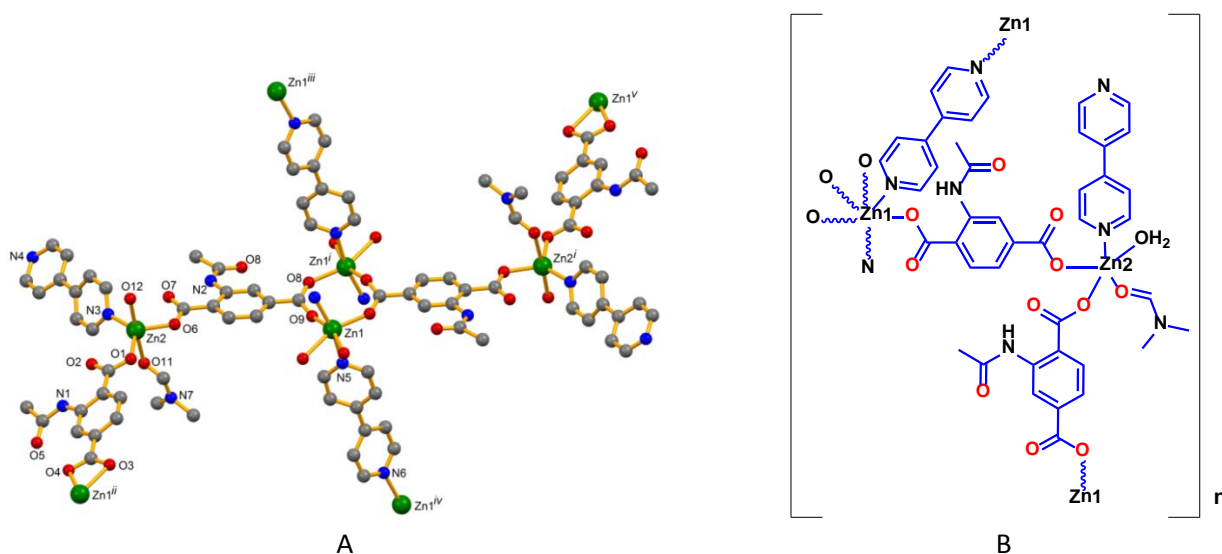
A

B

Figure 1: (A) Coordination scheme in **1** with partial atom labeling scheme. Hydrogen atoms were omitted for clarity. Symmetry operations to generate equivalent atoms: *i)* 1-x,1-y,-z; *ii)*1-x,1-y,1-z; *iii*) 1-x,2-y,-z; *iv*) x,-1+y,z.(B) Schematic representation of an asymmetric unit of **1**.

The Zn–O bond dimensions in **1** differ depending whether the oxygen atoms belong to bridging (the $L1^{2-}$ ligand moieties) or non-bridging ligands (water and DMF). The longest one pertains to DMF moiety [Zn2−O11] and the dimension that follows concern those of the chelating bidentate μ_1-O,O carboxylate group, with one of those bonds being considerably longer than the other [Zn1−O3 *vs.* Zn1−O4], followed by those involving the bridging bidentate μ_2-O,O' carboxylate [Zn1−O9 *vs.* Zn1−O8]. The Zn−O bonds involving the monodentate carboxylate moieties are the shortest ones found in this MOF [Zn2−O1 and Zn2−O6]. Expectedly, the Zn−N distances involving the bridging bipyridine are longer than those in the terminal one [2.154(3) and 2.048(4) Å, respectively].

Non-covalent interactions are present in **1** (Table S2). Concerning the N-H···O contacts, the amide groups of DMF intramolecularly donate to the non-coordinated O-carboxylate atoms, [d(D···A) distances of 2.611(5) and 2.616(4) Å], while the water molecule simultaneously donates to O_{amide} and to one of the chelating bidentate $O_{carboxylate}$ atoms [d(D···A) distances of 2.971(4) and 2.810(5) Å, respectively]. C−H···O contacts are also relevant; the strongest ones [d(D···A) distances in the 2.730(5) − 2.902(5) Å range] comprise the phenyl groups as donors and $O_{carboxylate}$ as acceptors, but also include the intramolecular DMF contact between one of the methyl hydrogen atoms and the carbonyl moiety (Table S8). Expectedly, several π···π stacking interactions are also present in these structures, the most relevant ones concerning contacts involving the Zn1-O3-C6-O4 metallacycle where the *centroid···centroid* distances can reach values as short as 3.714Å. Additionally, C−H···π contacts involve the C53 methyl of DMF as donor and the N6-containing pyridine groups of vicinal bridging bpy groups, and the C36 of these bpy groups as donors and the Zn1-O3-C6-O4 metallacycle as acceptor. These interactions present a minimum value of 2.700 Å, are considered as strong[41c], and may have influenced the larger twisted nature of these bridging ligands. These interactions help to stabilize the hydrogen bonded 3D structures of **1**.
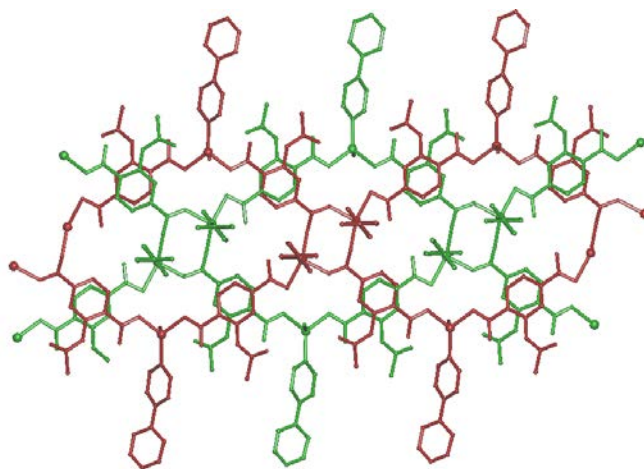
4

Figure 2: A representation of the 2-fold interpenetrated networks of **1** (one framework is represented in red and the other in green).

The hydrothermal reaction of 2-propionamidoterephthalic acid (H_2L2) with zinc (II) nitrate hexahydrate led to the formation of the 3D network $[Zn_4(L2)_3(OH)_2(DMF)_2(H_2O)_2]_n$ (**2**) (Figure 3A). Single-crystal X-ray diffraction studies reveal that **2** crystallizes in the monoclinic $P2_1/c$ space group and that the asymmetric unit contains two zinc(II) ions, one-and-a-half $L2^{2-}$ ligand, one bridging hydroxyl anion, one coordinated water molecule and one coordinated DMF molecule. The framework is built on tetranuclear μ_3-hydroxy-type clusters of $[Zn_4(OH)_2]^{3+}$ with a center of inversion in the middle of the $(Zn1)_2(OH)_2$ core (Figure 3B). Every tetranuclear connector is associated with six $L2^{2-}$ ligands, two molecules of water, two molecules of DMF and two μ_3-hydroxyl anions. While Zn1 has lightly distorted octahedral coordination geometry (OAV and OQE of 17.8 and 1.005, respectively)[41a] the Zn2 cation has a marginally distorted tetrahedral environment ($\tau_4 = 0.91$).[41d] The equatorial plane of Zn1 includes one of the O-atoms of a $L2^{2-}$ chelating carboxylate group, two bridging hydroxyl anions and the O-atom of the DMF molecule; the axial sites are occupied by a water molecule and the O-atom of another $L2^{2-}$ chelating carboxylate group. Consequently, the $L2^{2-}$ linked to the Zn1 metal cations can be considered to be in relative *cis*-position. The coordination sphere of Zn2 is fulfilled by the O-atom of a monodentate μ_1-$L2^{2-}$, other two O-atoms from two bridging μ_2-$L2^{2-}$ ligands and a water molecule. The Zn–O bond distances range from 1.928(3) to 2.113(2) Å, but those involving Zn2 do not exceed 1.967(3) Å, and concerning Zn1 do not go below 2.070(3) Å; in any case, the longer bonds regard the bridging hydroxyl moiety. The shortest Zn···Zn distance in the structure is of 3.1250(7) Å which involves Zn1 and the peripheral Zn2 ions; the symmetry related Zn ions, in turn, are slightly further apart [3.1759(6)Å].
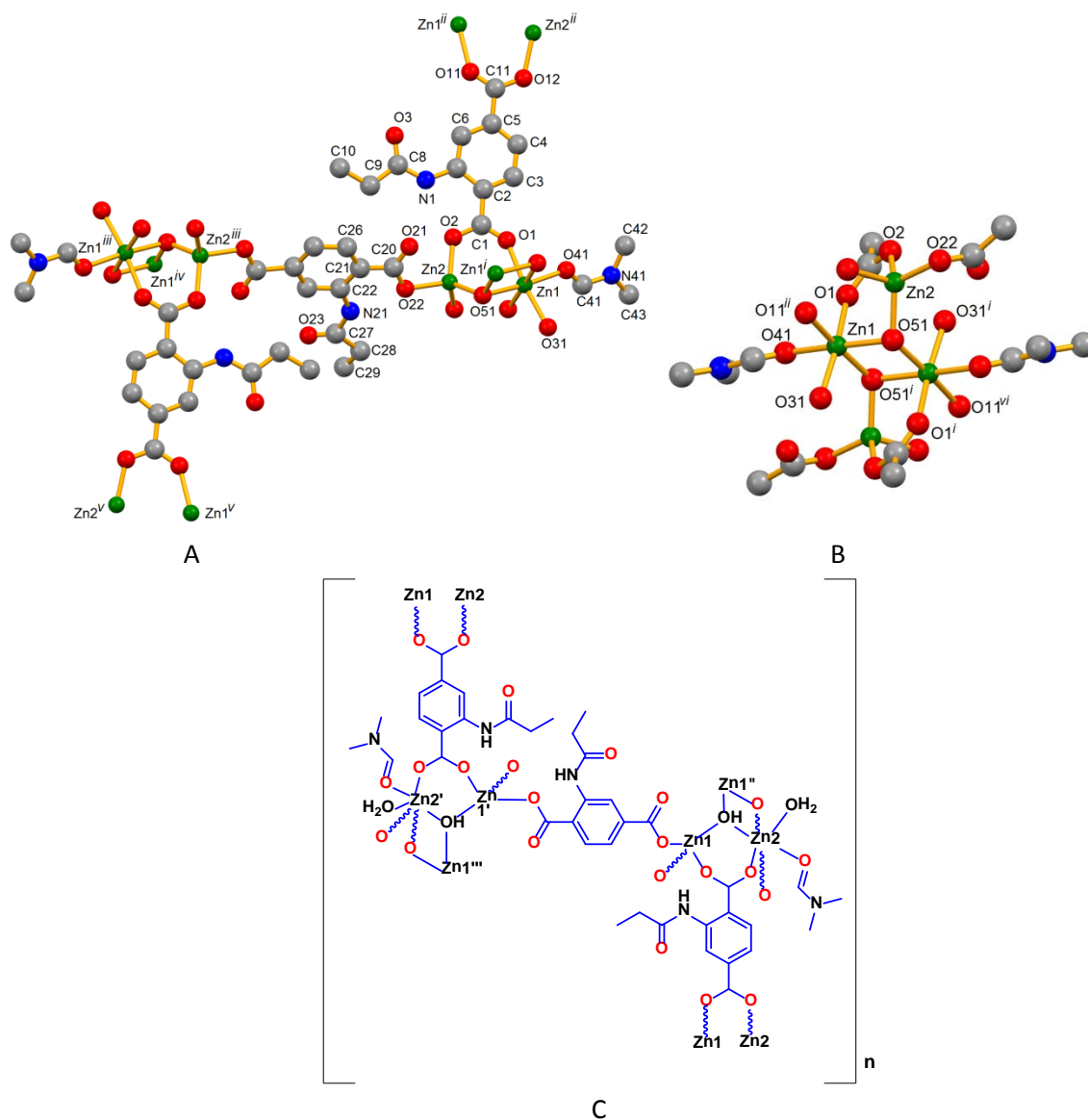
Figure 3: (A) Coordination scheme in **2** with partial atom labeling scheme. Hydrogen atoms are omitted for clarity. (B) Basic structure of the dihydroxo-bridged Zn-tetramer $[Zn_4(OH)_2]^{3+}$ unit showing the metal coordination spheres. Symmetry operations to generate equivalent atoms: *i*) 2-x,2-y,1-z; *ii*) 2-x,-1/2+y,1.5-z; *iii*) 1-x,2-y,1-z; *iv*) -1+x,y,z; *v*) -1+x,2.5-y,-1/2+z; *vi*) x,1.5-y,-1/2+z. (C) Schematic representation of an asymmetric unit of **2**.
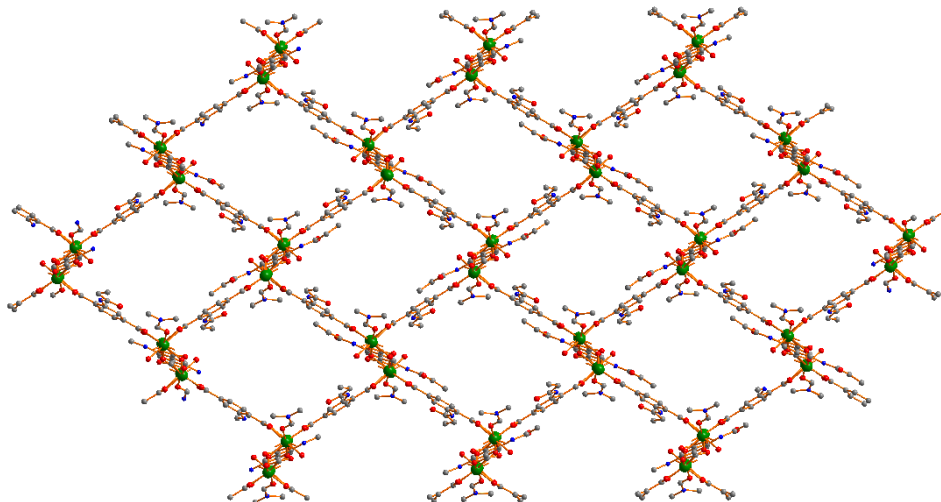
Figure 4: A representation of the 3D network of **2**.

The packing view of **2** is characterized by open channels along the crystallographic *a* axis (Figure 4) with approximate dimension of 10.45 x 7.67 Å^2, measured as the distance between the H10C-methyl and the H29C-methyl groups of the L2^{2-} ligands, respectively. The structure of **2** is also stabilized by hydrogen bonding interactions (Table S2), the most significant one involving the coordinated water molecule (O31) as donor to the carboxylate oxygen atom O21. The amide H-atoms also interact with carboxylate moieties. Moreover, intermolecular C−H···O contacts are relevant and help to stabilize the structure.

Single-crystal X-ray diffraction studies reveal that [Zn(L3)(H$_2$O)$_2$]$_n$. n/2(1,4-dioxane) (**3**) crystallizes in the monoclinic P2$_1$/c space group, and that the asymmetric unit contains one zinc(II) ions, one L3^{2-} ligand, two coordinated water molecules (Figure 5) and a free 1,4-dioxane fragment. Compound **3** features a zig-zag type one-dimensional coordination polymeric chain, but expands to 3D by means of H-bond interactions. The Zn1 center presents a presents a distorted tetrahedral environment (τ_4 = 0.87)[41d] and binds to two carboxylate oxygen atoms of two neighboring L3^{2-} units in a monodentate fashion [Zn1−O1 and Zn1−O3] and to two water molecules [Zn1−O10 and Zn1−O20]. In this framework the organic ligand is almost planar the maximum deviations from its mean least square plane pertaining to the O4 and O3 atoms (0.181 and 0.172 Å, respectively), the metal atom being shifted 0.143 Å from it. The presence of a phenyl ring in the side functionality of the L3^{2-}ligand prevented the formation of a structure with a higher dimensionality, and a 1D zig-zag chain is formed instead (Figure 5). However, the intermolecular organization in the crystal is characterized by hydrogen bonding interactions involving the carboxylate groups as acceptors and the coordinated water molecules, as well as the dioxane molecule as donors (Table S2), expanding the structure to the third dimension (Table S2).
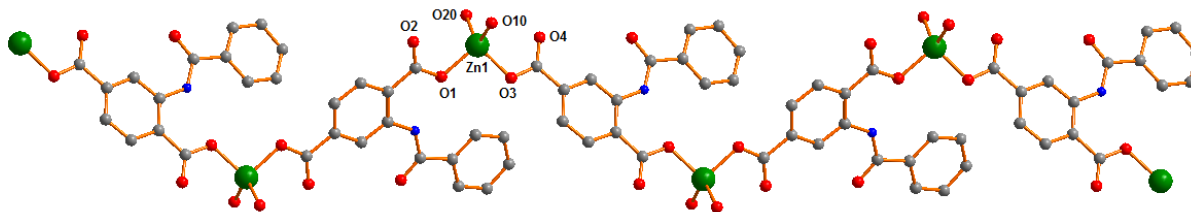
Figure 5: One dimensional zig-zag structure of **3** with partial atom labeling scheme. Symmetry operations to generate equivalent atoms: *i*)-1+x, 1/2-y, -1/2+z; *ii*)1+x, 1/2-y, 1/2+z; *iii*) -2+x, y, -1+z; *iv*) 2+x,y,1+z.

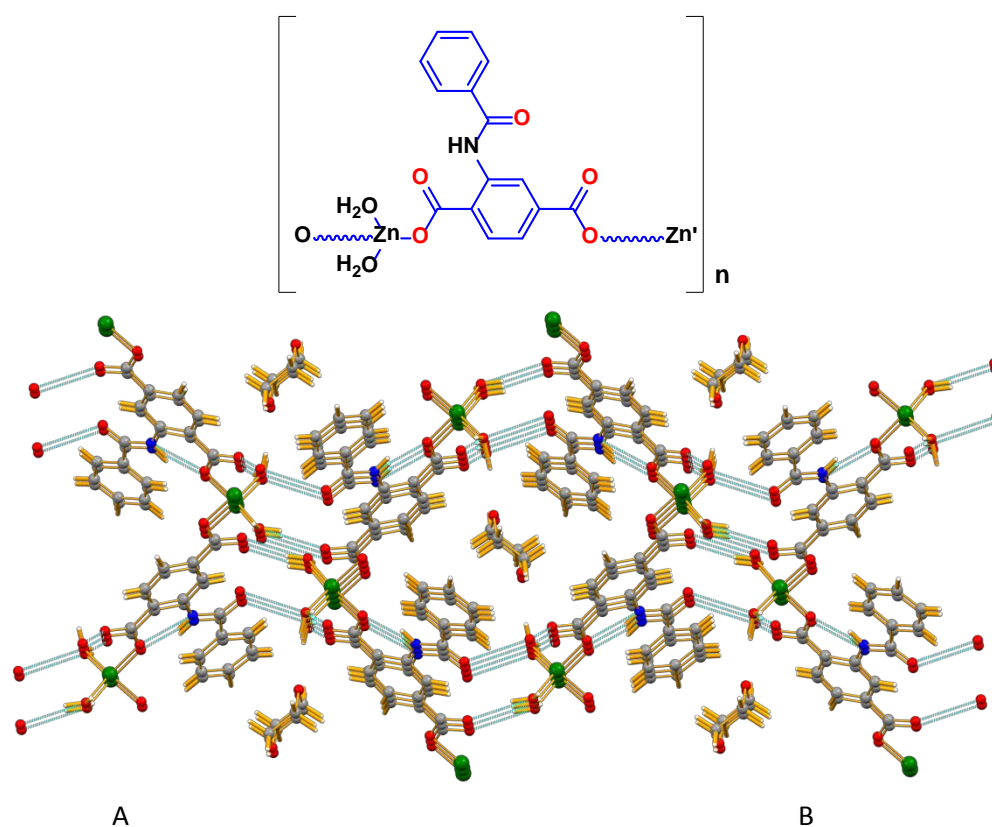A   B

Figure 6: (A) Schematic representation of an asymmetric unit of **3**. (B) Hydrogen bonded networks of **3** with hydrogen bonding interaction drawn in cyan dotted lines.

One may conclude from the above observations that the three dicarboxylic ligands H_2L1, H_2L2 and H_2L3 reveal different coordination features in the coordination polymers with zinc(II) metal ions, and the amide substituents play a significant role. The more bulky amide side functionality produces a low dimensional framework. Three different ligands produce three different structures which are not only depend upon the reaction conditions but also on the auxiliary ligands.

8

Topological analysis

To improve the description of the crystal structures of **1**, **2** and **3** we performed their topological analysis by reducing their multidimensional structures to simple node-and-linker nets where the metallic nodes and the organic linkers represent secondary building units (SBUs).[42] We have carried out these analyses by using TOPOS 4.0.[42c] In order to do so we have removed the entire lattice and coordinated solvent molecules from the frameworks. In the particular case of **1** where Zn2 is mono coordinated via carboxylate ligands and Zn1 forms a binuclear cluster via bridging carboxylates, we considered the latter as a single node subsequently coordinated via 8 different carboxylates and bipyridine linker; the Zn2 ion, being connected to two ligand moieties, represents a 2-connected node. Relative to the $L1^{2-}$ ligand and the 4,4'-bipyridine, both connected to Zn1 and Zn2, they act as 2-connected nodes. The polymeric chain structure thus generated is a 4-nodal (2,2,2,8)-connected net with the Schläfli symbol $\{6^2.8^2.14^{16}.20^4.22^4\}\{6\}_4\{8\}_6$. Moreover, this network also has two different interpenetrated nets (Figure 7A).
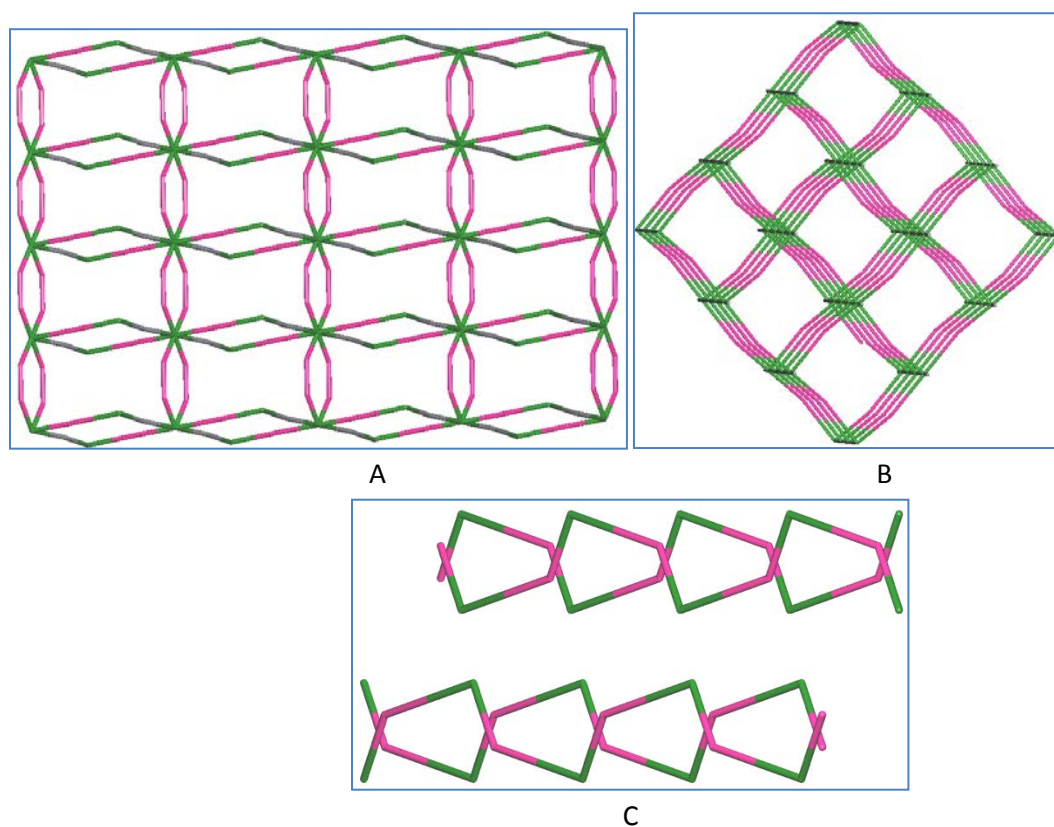

Figure 7: Node-and-linker-type descriptions of the 2D coordination frameworks in **1** (A), of the 3D coordination frameworks in **2** (B), and of the 1D coordination frameworks in **3** (C).The metal nodes are represented in green and the linkers in pink color.

MOF **2** can be represented as a complex (2,6)-connected binodal net, with the Schläfli symbol $\{8^{12}.12^3\}\{8\}_3$ and 2,6T1 type topology (binary.ttd). In this framework the tetranuclear zinc cluster serves as a single node coordinated via six $L2^{2-}$ ligands which, in turn, is connected to two Zn centers (Figure

7B). The 1D of **3** represents binodal (2)-connected nets which result from the metal coordination to two L3^{2-} ligands in line connected with two Zn centers (Figure 7C).

Thermogravimetric analyses

Thermogravimetric analyses were carried out under dinitrogen from room temperature to *ca*. 650 ºC at a heating rate of 10 ˚C min^{-1}. Features of the thermal stability of the frameworks are illustrated in Figure 8.

1 shows weight loss of 9.2% between 180 and 250 ˚C, corresponding to the loss of one molecule of water and one molecule of DMF (calcd: 9.3%). Upon further heating, the anhydrous compound is stable up to 342 ˚C but in the temperature range of 342 to 517˚C it shows a weight loss of 61.1%, which corresponds to two molecules of 4,4'-bipyridine and one ligand (L1) (calcd: 60.6%).

2 exhibits a weight loss of 15.0% in the 37-294 ˚C temperature range, which accounts for the total removal of one water and one DMF molecules from the coordination sphere of the metal (calcd: 15.4%). The remaining material then decomposes gradually until 550 ºC.

3 loses 10.7% of its weight between 117 and 175 ˚C, most likely due to de-sorption of 1,4-dioxane (calcd: 10.3%). The residue remains stable up to about 247 ˚C and then releases two coordinated water molecules until 351 ˚C, which corresponds to weight loss of 8.9% (calcd. weight loss 9.3%) and then gradually decomposes until 550 ˚C.
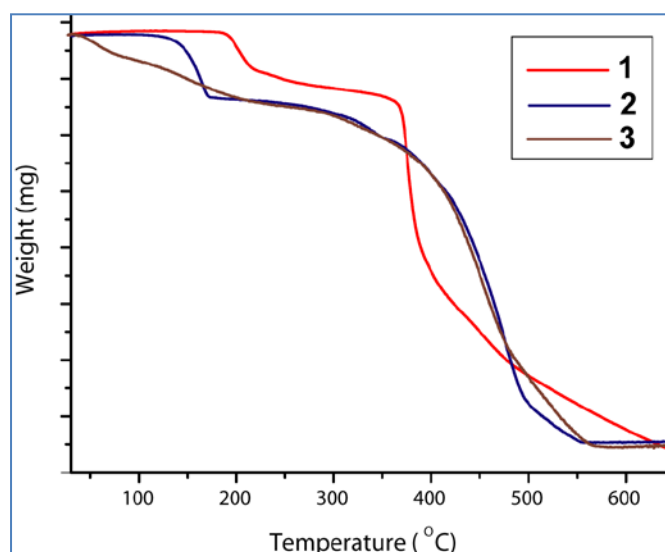
Figure 8: Thermogravimetric curves for **1**, **2** and **3**.

Catalytic activities towards the Henry reaction

We have tested the potential catalytic activity of frameworks **1**, **2** and **3** as solid heterogeneous catalysts in the nitroaldol (or Henry) reaction of nitroethane with various aldehydes. In a typical reaction, a mixture of aldehyde (0.5 mmol), nitroethane (0.3mL) and Zn catalyst (3 mol %) in 2mL MeOH, contained in a capped glass vessel, was stirred at 70ºC for 48 h, whereupon the solution was filtered to remove the

catalyst. The solvent was evaporated in vacuum, giving the crude product as a mixture of the β-nitroalkanol diastereoisomers (*syn* and *anti* forms, with predominance of the former) which were analyzed by ^{1}H NMR (see Supplementary Information file).

By using benzaldehyde as a test compound, we found that **1** showed a higher conversion as compared to **2** and **3** after the same reaction time and at the same temperature. Consequently, the optimization of the reaction conditions (temperature, reaction time, amount of catalyst and solvent) was carried out in a model nitroethane–benzaldehyde system with **1** as the catalyst precursor (Scheme 2 and Table 1).

Scheme 2: Nitroaldol (Henry) reaction
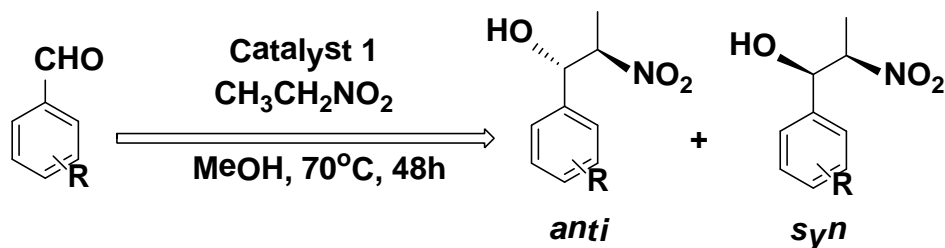
Blank reactions were also performed (absence of any metal source; Table 1, entry 21) using benzaldehyde as substrate, at 70 ºC and in methanol. No β-nitroalkanol was detected after a reaction time of 48 h. The nitroaldol reaction also did not take place when using $Zn(NO_3)_2$ or compound H_2L1 instead of catalyst **1** (Table 1, entries 22 and 23, respectively). However, when 3mol% of **1** is used as catalyst, a conversion of 95% (*anti*:*syn* = 27:73) of benzaldehyde into β-nitroalkanol is reached (entry 9, Table 1). With **2** and **3** a conversion of 83% (*anti*:*syn* = 31:69) and 91% (*anti*:*syn* = 32:68) were obtained, respectively (entries 19 and 20, Table 1). Extending the reaction time to 72 h did not increase the yield of the reaction. The plots of yield *versus* time for the Henry reaction of benzaldehyde and nitroethane catalysed by **1**, **2** and **3** are presented in figure 9A. The observed high conversion rate in the case of **1** directs it as an efficient catalyst for this reaction.
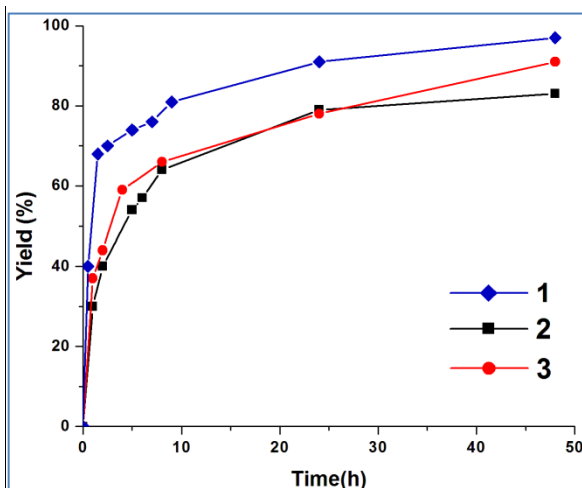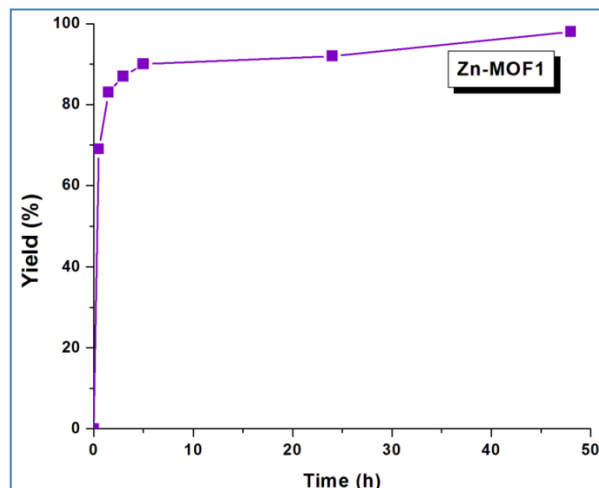
A   B

Figure 9: (A) Plots of β-nitroalkanol yield *vs.* time for the Henry reaction of benzaldehyde and nitroethane with **1** (♦), **2** (■) and **3** (●). (B) Plots of β-nitroalkanol yield *vs.* time for the Henry reaction of 4-nitro benzaldehyde and nitroethane with **1**.

Table 1: Optimization of the parameters of the Henry nitroaldol reaction between benzaldehyde and nitroethane with **1** as the catalyst

Entry	Catalyst	Time (h)	Amount of Catalyst (mol%)	T (°C)	Solvent	Yield (%)	Selectivity (*anti/syn*)	TOF (h^{-1})
1	**1**	0.5	3.0	70	MeOH	40	27:73	26.7
2	**1**	1.5	3.0	70	MeOH	68	28:72	15.1
3	**1**	2.5	3.0	70	MeOH	70	28:72	9.3
4	**1**	5	3.0	70	MeOH	74	27:73	4.9
5	**1**	7	3.0	70	MeOH	76	26:74	3.6
6	**1**	9	3.0	70	MeOH	81	26:74	3.0
7	**1**	24	3.0	70	MeOH	91	27:73	1.3
8	**1**	48	1.0	70	MeOH	48	24:76	1.0
9	**1**	48	3.0	70	MeOH	95	27:73	0.7
10	**1**	48	5.0	70	MeOH	70	22:78	0.3
11	**1**	48	7.0	70	MeOH	71	25:75	0.2
12	**1**	48	3.0	70	THF	40	25:75	0.3
13	**1**	48	3.0	70	H_2O	78	20:80	0.5
14	**1**	48	3.0	70	CH_3CN	-	-	-
15	**1**	48	3.0	RT	MeOH	20	26:74	0.14
16	**1**	48	3.0	30	MeOH	46	25:75	0.3
17	**1**	48	3.0	50	MeOH	70	26:74	0.5
18	**1**	48	3.0	100	MeOH	45	31:69	0.3
19	**2**	48	3.0	70	MeOH	83	31:69	0.6
20	**3**	48	3.0	70	MeOH	91	32:68	0.64
21	Blank	48	-	70	MeOH	-	-	-
22	$Zn(NO_3)_2.6H_2O$	48	3.0	70	MeOH	-	-	-
23	H_2L1	48	3.0	70	MeOH	-	-	-
24[a]	**1**	48	3.0	70	MeOH	84	29:71	0.6
25[b]	**1**	48	3.0	70	MeOH	51	16:74	0.4
26[c]	**1**	48	3.0	70	Solvent free	64	24:76	0.4

[a] Nitromethane was used as substrate; [b] Nitropropane was used as substrate; [c] Methanol (solvent)-free conditions, using nitroethane as solvent (2 mL).

We have also tested the effect of temperature, catalyst amount and solvents in the Henry reaction. An increase of the catalyst amount from 1.0 and 3.0 mol% enhances the product yield from 48 to 95%, respectively (entries 8 and 9, Table 1), but further rise decreases the reaction yield to 70% (entries 10 and 11, Table 1). We have also examined the effect of different solvents in this reaction (entries 12– 14, Table 1). The reaction did not proceed in acetonitrile, and in THF only 40% total yield was achieved. If nitroethane was used as solvent (added solvent-free conditions, entry 26), 64% yield was attained. By using a polar solvent (MeOH or H_2O) the yields increased up to 95 and 78%, respectively (entries 9 and 13, Table 1). These results point out the possible role of protic and polar solvents in the proton transfer process of the nitroaldol reaction[34j-34l]. Ranging the temperature from 20 to 70 ºC improved the yield of β-nitroalkanol from 20 to 95% but further increase in the reaction temperature had a negative effect (entries 9 and 15–18, Table 1).The systems exhibit diastereoselectivity towards the *syn* isomer, typically leading to *syn*:*anti* molar ratios in the range of 80:20 to 68:32 using nitroethane as substrate. The size of the nitroalkane chain also affects the yields; while with nitropropane the conversion was only of 51% (entry 25, Table 1) with nitroethane or nitromethane values of 95% or 84% were obtained (entries 9 or 24, Table 1).

Although there are some reports on coordination polymers[35] which are catalytically active for this kind of reaction, the yields and selectivity are usually higher for our compounds as compared to other metal organic frameworks (Table 2). The 3D zinc(II) framework with 1,3,5-tri(4-carboxyphenoxy)benzene, in the reaction of 4-nitrobenzaldehyde and nitroethane, leads to an overall yield of only 15% after 72 h reaction time (Table 2);[35a] with a 1,4-diazabicyclo[2.2.2]octane (DABCO) functionalized 3D-Zn MOF an yield of 34% after 120 h was obtained (Table 2).[35b] Moreover, our catalyst **1** exhibits a marked selectivity towards the *syn* diastereoisomer (Table 2, *syn:anti*=78:22) which was not reported in other cases.
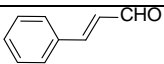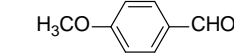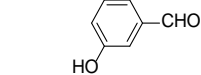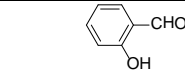
Table 2: Comparison of activities of MOFs as catalysts for the Henry reaction with an aldehyde and nitroethane					
Catalyst	Solvent/Temp/Time	Aldehyde	Yield (%)	Selectivity *syn*/*anti*	Reference
1	MeOH/70˚C/48h	4-Nitrobenzaldehyde	98	78:22	This work
Zn(II) MOF with 1,3,5-tri(4-carboxyphenoxy)benzene	Solvent free/70˚C/72h	4-Nitrobenzaldehyde	15	Not determined	35a
Zn(II) MOF with terphenyl-3,3,-dicarboxylate and 1,4-diazabicyclo[2.2.2]octane (DABCO)	Solvent free/60˚C/120h	4-Nitrobenzaldehyde	34	Not determined	35b
Cu(II) MOF withpyridine carboxylates	Solvent free/70˚C/36h	4-Nitrobenzaldehyde	78	Not determined	35c

We have also compared the activities of the three Zn(II) frameworks in the reactions of a variety of *para-* or *ortho*-substituted aromatic and aliphatic aldehydes with nitroethane, producing the corresponding β-nitroalkanols with yields ranging from 21 to 98% (Table 3).The reactivity of **1** is generally higher than those of **2** and **3** and this may result from the greater Lewis acid nature of the former, a factor that should promote the H$^+$-nitroalkane bond cleavage and the electrophilicity of the aldehyde, thus favoring the global reaction (scheme 3).

The nature of the substrates is an important factor. Indeed, aryl aldehydes bearing electron-withdrawing groups exhibit higher reactivities (Table 3, entries 2 and 4) as compared to those having electron-donating moieties, what may be related with an increase of the electrophilicity of the substrate in the former case.

Table 3: Henry reaction of various aldehydes and nitroethane with catalysts **1**, **2** and**3**				
Entry	Compounds	Yield (%) by using **1**	Yield (%) by using **2**	Yield (%) by using **3**
1	⌬—CH=CH—CHO	96	79	69
2	O_2N—⌬—CHO	98	96	98
3	H_3CO—⌬—CHO	39	21	26
4	Cl—⌬—CHO	93	84	90
5	H_3C—⌬—CHO	62	31	51
6	⌬—CHO (HO)	83	47	71
7	⌬—CHO (OH)	52	21	40
8	CH_3CHO	98	84	97
9	CH_3CH_2CHO	91	75	92

In order to examine the lifetime and stability of **1** in the Henry reaction, the catalyst was recycled in two consecutive experiments. The observed activity was kept over the two cycles of reaction with just a slight decrease in the second run (Figure 9). The FT-IR spectra of the catalyst **1** taken before and after the reaction did not indicate any important changes (Supporting information, Figure S2A), suggesting the integrity of the polymeric structure of the solid. This fact is also sustained by PXRD also performed before and after the Henry reaction (Supporting information, Figure S3A). Recycling experiments for **2** and **3** were also undertaken confirming that these frameworks also remain active after the reactions (Supporting information, Figure S1). The FT-IR spectra of the catalysts **2** and **3** before and after the reaction also did not indicate any important changes (Supporting information, Figure S4)

14
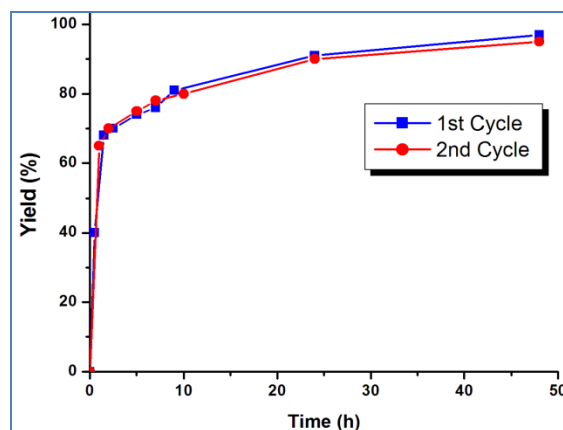
Figure 9: Kinetic profiles in two consecutive reaction cycles employing **1** as catalyst.

A proposed catalytic cycle for the Henry reaction catalyzed by **1** is presented in Scheme 3. The activation of both the aldehyde and the nitroethane by the metal centre is followed by the formation of C-C bond upon electrophilic addition leading to the formation of β-nitroalkanol[34b], following processes that appear to be favored by the electrophilicity of the aldehyde and by the protic and polar characters of the solvent.
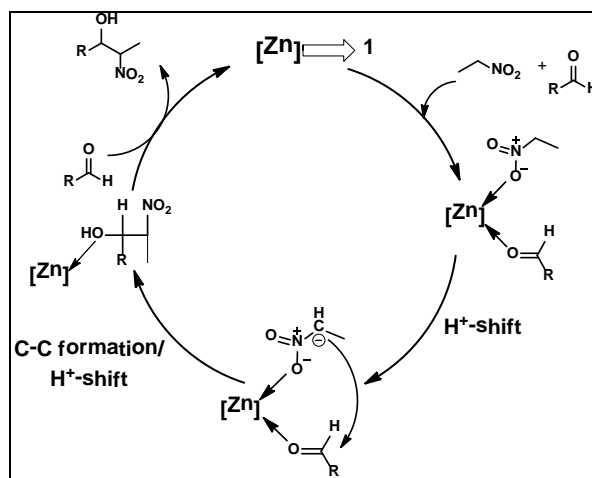
Scheme 3: Proposed catalytic cycle for the formation of the β-nitroalkanol in Henry reaction catalyzed by **1**.

Catalytic activity in the transesterification reaction

In a typical reaction, a mixture of methyl-3-nitrobenzoate (0.5 mmol) and catalyst **2** (3 mol %) in 2 mL EtOH was added into a capped glass vessel, and the resulting mixture was stirred at 100 ºC for 24 h. The solution was filtered to remove the catalyst and the solvent was evaporated in vacuum, leading to a crude mixture of products which was analyzed by ^{1}H NMR (see Supplementary Information file). Since our frameworks have very low solubility in alcohols, they are potentially good candidates for heterogeneous catalytic transesterification of nitrobenzoates.

Entry	Catalyst	Time (h)	Amount of catalyst (mol%)	T (℃)	Solvent	Yield (%)	TON	TOF (h^{-1})
1	**2**	1	3.0	100	EtOH	5.5	1.8	1.8
2	**2**	2	3.0	100	EtOH	9	3.0	1.5
3	**2**	3.5	3.0	100	EtOH	40	13.3	3.8
4	**2**	6	3.0	100	EtOH	56	18.6	3.1
5	**2**	10	3.0	100	EtOH	76	25.3	2.5
6	**2**	24	3.0	100	EtOH	97	32.3	1.3
7	**2**	48	3.0	100	EtOH	97	32.3	0.7
9	**2**	24	1.0	100	EtOH	94	31.5	1.3
10	**2**	24	5.0	100	EtOH	97.1	32.5	1.3
11	**2**	24	7.0	100	EtOH	96	32.1	1.3
12	**2**	24	3.0	100	1-PrOH	64	21.4	0.9
13	**2**	24	3.0	100	2-PrOH	44	14.7	0.6
14	**2**	24	3.0	RT	EtOH	2.0	0.7	0.03
15	**2**	24	3.0	50	EtOH	11	3.7	0.15
16	**2**	24	3.0	75	EtOH	51	17.1	0.7
17	**2**	24	3.0	120	EtOH	96	32.4	1.4
18	**1**	24	3.0	100	EtOH	37	12.3	0.5
19	**3**	24	3.0	100	EtOH	34	11.3	0.47
20	Blank	24	-	100	EtOH	-	-	-
21	$Zn(NO_3)_2.6H_2O$	24	3.0	100	EtOH	10	3.3	0.14
22	Ligand H_2L2	24	3.0	100	EtOH	-	-	-

Table 4: Optimization of the parameters of the transesterification reaction of methyl-3-nitrobenzoate in ethanol with **2** as catalyst

When 3 mol% of solid **2** is used as catalyst, a conversion of 97% of methyl-3-nitrobenzoate into ethyl-3-nitrobenzoate is reached after 24 h reaction time (entry 6, Table 4). The yield *vs.* time plot for the transesterification reaction of methyl-3-nitrobenzoate and ethanol using **2** as catalyst is shown in Figure 10. In a similar reaction using **1** and **3**, conversions of 37% and 34% (entries 18 and 19, Table 4) were obtained, respectively, after 24 h. Extending the reaction time to 48 h did not increase the yield. The high conversion rate suggests that **2** act as a more efficient catalyst as compared with **1** and **3** for the transesterification reaction. Thus, the optimization of the reaction conditions (temperature, reaction time, amount of catalyst and solvent) was performed using **2** as the catalyst (Scheme 4).
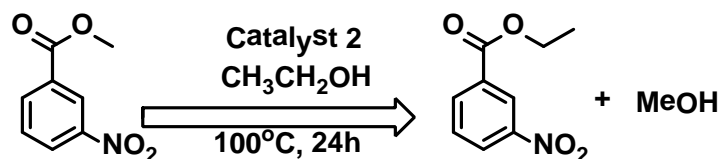
Scheme 4: Transesterification reaction

The increase of the catalyst amount slightly enhances the product yield from 94 to 97% for the corresponding amounts of 1.0 and 3.0 mol% of catalyst **2**, but a further increase in the catalyst amount to 7 mol% did not improve the yield (entries 9-11 and 6, Table 4). When 1-propanol was used as solvent instead of ethanol the reaction yield decreased from 97 to 64% (compare entries 6 and 12, Table 4). The reaction conversion further decreased to 44 % with the use of a secondary alcohol (2-propanol entry 13, Table 4). Increasing the reaction temperature from room temperature to 100 ºC increased the yield of the reaction from 2 to 97% but a further rise in the temperature led to a decrease in the overall yield (compare entries 11, 14–17, Table 4). No product was detected when the reaction was performed in the absence of the catalyst and keeping the same experimental conditions (entry 20, Table 4). Control reactions were also carried out using $Zn(NO_3)_2$ as catalyst and a 10% conversion was reached after 24h (entry 21, Table 4). No transesterification occurred when H_2L2 was used instead of the catalyst (entry 22, Table 4).
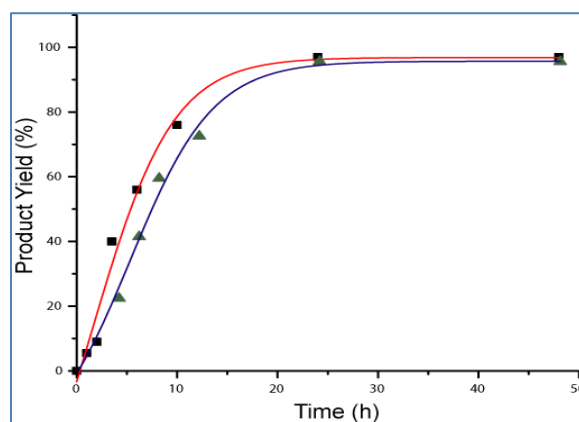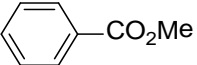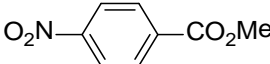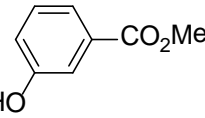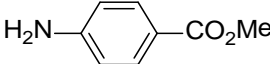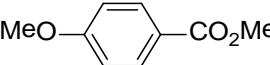
Figure 10: Plots of product yield *vs.* time (two consecutive reaction cycles) for the transesterification reaction of methyl-3-nitrobenzoateand ethanol with **2**.

Once having established that compound **2** represents an excellent catalyst for the transesterification transformation, we investigated the reaction of various substituted methyl benzoates in ethanol. The substrate with an electron-withdrawing substituent underwent fast transesterification (Table 5, entry 2) whereas those with electron-donating groups experienced a slower conversion (Table 5, entries 3-5). Methyl benzoate also converted to ethyl benzoate with a yield of 73%.

Table 5: Transesterification reaction of various methyl esters with **2** as catalyst								
Entry	Substrate	Time (h)	Amount (mol%)	Solvent	T (°C)	Yield (%)	TON	TOF (h^{-1})
1	⬡—CO$_2$Me	24	3%	EtOH	100	73	24.3	1.0
2	O$_2$N—⬡—CO$_2$Me	24	3%	EtOH	100	96	32.4	1.4
3	⬡—CO$_2$Me (HO)	24	3%	EtOH	100	51	17.0	0.7
4	H$_2$N—⬡—CO$_2$Me	24	3%	EtOH	100	76	24.4	1.0
5	MeO—⬡—CO$_2$Me	24	3%	EtOH	100	48	16.0	0.6

In order to examine the recyclability of catalyst **2**, we removed it by filtration after the transesterification reaction of methyl-3-nitrobenzoate, dried it and reused it as catalyst in a subsequent transesterification process observing just a slight decrease in reactivity (Figure 10). FT-IR spectra of **2** taken before and after the reaction (Supporting Information, Figure S2B) did not indicate any important changes. This fact is also sustained by PXRD performed before and after the transesterification reaction (Supporting information, Figure S3B). This suggests that the integrity of catalyst **2** was retained after reaction. Additionally, the filtrate solution, after the separation of the catalyst, was taken to dryness and the amount of zinc determined, being only 0.09% of the amount used in the reaction, thus ruling out any significant leaching of the catalyst.

The mechanism of metal catalyzed transesterification probably involves an electrophilic activation of the carbonyl moiety of the substrate upon binding to the metal centre of the catalyst.[44] Accordingly the Lewis acidity of this centre may be relevant in this catalytic reaction. A possible transesterification mechanism is shown in Figure 11.
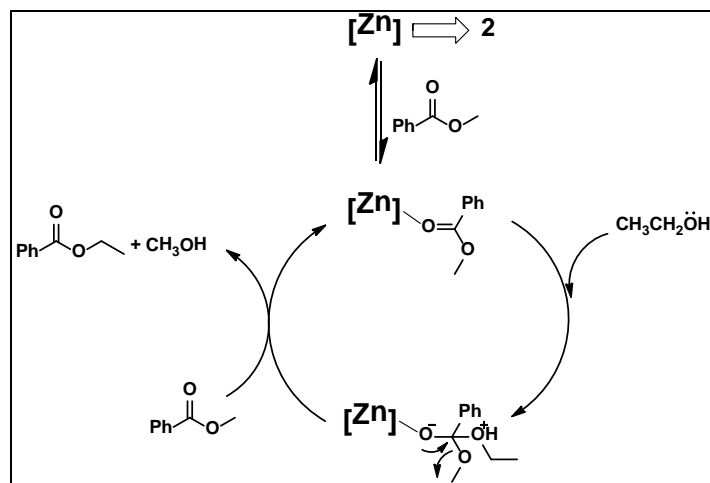

Figure 11: Proposed catalytic cycle for the transesterification reaction catalyzed by **2**.

18

Concluding remarks

The synthesis and characterization of three novel amido terephthalic acids having different hanging side functionalities are reported. These compounds led successfully to one, two and three dimensional coordination polymers upon reaction with zinc(II) metal ions. The structures of the new frameworks have been determined by single crystal X-ray diffraction analysis. The construction of the multidimensional structures was facilitated by the hanging side functionality of the ligands, where the amide substituents appeared to play a significant role as the bulkier moiety produced a lower dimensional framework; a dependence on the reaction conditions and on the auxiliary ligand could also be recognized. Accordingly, i) a 1D coordination polymer (**3**) of the zinc ions could be obtained with the L3^{2-} ligand, the one with the largest amide group; ii) direct binary reactions of L1^{2-} with zinc(II) did not lead to a crystalline polymeric aggregate, but a 2D framework (**1**) could be obtained with bipyridine as auxiliary ligand; iii) the combination of L2^{2-} with zinc ions produced a 3D framework (**2**) with channels along the crystallographic *a* axis.

Taking advantage of the lack of solubility of the synthesized zinc frameworks in alcohols and other common solvents they were tested as heterogeneous catalysts for nitroaldol (Henry) and transesterification reactions. Framework **1** was the most effective catalyst for the Henry reaction of nitroethane with various aldehydes producing the corresponding β-nitroalkanols in high yields and with a significant stereoselectivity towards the *syn* diastereomer. The yields of the nitroaldol reaction were found to increase with the electrophilicity of the substrates, the protic nature and polar character of the solvent also playing an important role. Framework **2** was the most effective catalyst for the transesterification of a variety of esters with different alcohols.

The above observations provide evidence that MOFs can be utilized as effective heterogeneous catalysts in important types of reactions. Further explorations into the uses of this type of MOFs as catalysts in other organic transformations, as well as mechanistic investigations, are ongoing.

Experimental

The synthetic work was performed in air and at room temperature. All the chemicals were obtained from commercial sources and used as received. The infrared spectra (4000–400 cm^{-1}) were recorded on a BIO-RAD FTS 3000 MX instrument in KBr pellets; abbreviations: s = strong, m = medium, w = weak, bs = broad and strong, mb = medium and broad. The ^{1}H and ^{13}C NMR spectra were recorded at ambient temperature on a Bruker Avance II + 300 (UltraShield™ Magnet) spectrometer operating at 300.130 and 75.468 MHz for proton and carbon-13, respectively. The chemical shifts are reported in ppm using tetramethylsilane as the internal reference; abbreviations: s = singlet, d = doublet, t = triplet, q = quartet. Carbon, hydrogen and nitrogen elemental analyses were carried out by the Microanalytical Service of the Instituto Superior Técnico. Electrospray mass spectra (ESI-MS) were run with an ion-trap instrument (Varian 500-MS LC Ion Trap Mass Spectrometer) equipped with an electrospray ion source. For electrospray ionization, the drying gas and flow rate were optimized according to the particular sample with 35 p.s.i. nebulizer pressure. Scanning was performed from *m/z* 100 to 1200 in methanol solution. The compounds were observed in the positive mode (capillary voltage = 80–105 V). Thermal

properties were analyzed with a Perkin-Elmer Instrument system (STA6000) at a heating rate of 10°C min^{-1} under a dinitrogen atmosphere. Powder X-ray diffraction (PXRD) was conducted in a D8 Advance Bruker AXS (Bragg Brentano geometry) theta-2theta diffractometer, with copper radiation (Cu Kα, λ = 1.5406 Å) and a secondary monochromator, operated at 40 kV and 40 mA. Flat plate configuration was used and the typical data collection range was between 5° and 40°.

Synthesis of 2-acetamidoterephthalic acid (H$_2$L1)

A 1.81 g (10 mmol) portion of 2-aminoterephthalic acid was dissolved in 10 mL of acetic anhydride and the reaction mixture was refluxed for 4 h at 80 ºC, after which 20 mL of water were added and the solution further heated until boiling. The obtained white solid product of 2-acetamidoterephthalic acid (**H$_2$L1**) was filtered off and washed with water until total removal of acetic acid. Yield: 82% (1.83 g). Anal. Calcd. for C$_{10}$H$_9$NO$_5$ (*M* = 223.18): C, 53.82; H, 4.06; N, 6.28. Found: C, 53.15; H, 4.10; N, 6.50. FT-IR (KBr, cm^{-1}):3138 (bs), 2579 (mb), 1693 (s), 1581 (s), 1535 (s), 1466 (m), 1424 (s), 1386 (m), 1285 (s), 1196 (s), 1150 (w), 1019 (w), 971 (s), 936 (w), 803 (w), 759 (s), 668 (w), 554 (w), 504 (w); ^{1}H-NMR (DMSO-d^6): 10.98 (1H, s, -NH), 8.98 (1H, s, Ar-H), 8.03 (2H, d, 8.4Hz, Ar-H), 7.64 (2H, d, 8.4Hz, Ar-H), 2.14 (3H, s, -CH$_3$); ^{13}C-NMR (DMSO-d^6): 172.5, 168.7, 166.5, 140.5, 135.2, 131.2, 123.0, 120.9, 120.4, 24.9. MS (ESI): *m/z*: 246.0 [M+Na]$^+$.

Synthesis of 2-propionamidoterephthalic acid (H$_2$L2)
This compound was synthesized by a two-step procedure.
In the first step, dimethyl-2-aminoterephthalate (2.09 g, 10 mmol) and NEt$_3$ (1.51 g, 15 mmol) were placed in a round bottom flask and then dry dichloromethane (20 mL) was added. After cooling in an ice bath followed by dropwise addition of propionyl chloride (1.10 g, 12 mmol) the reaction mixture was stirred overnight at room temperature. Upon removal of the solvent under reduced pressure a yellow solid was obtained. 20 mL of water were added to the yellow solid which was then extracted with dichloromethane. The organic extracts were collected over anhydrous sodium sulfate; subsequent removal of the solvent gave the methyl ester of compound H$_2$L2. Yield: 73% (1.93 g).
In the second step, the isolated ester (2.65 g, 10 mmol) and NaOH (0.8 g, 20 mmol) were dissolved in 20 mL of MeOH : water (4 : 1). The reaction mixture was refluxed for 4 h at 80 °C, after which the solvent was removed under reduced pressure, 10 mL of water were added and the solution was acidified (pH=2) with dilute HCl solution. The obtained yellow solid product H$_2$L2 was removed by filtration and washed with water until total removal of the acid. Yield: 62% (1.47 g). Anal. Calcd. for C$_{11}$H$_{11}$NO$_5$ (M = 237.21): C, 55.70; H, 4.67; N, 5.90. Found: C, 55.35; H, 4.50; N, 5.62.FT-IR (KBr, cm^{-1}): 3345 (bs), 2978 (mb), 2560 (mb), 1683 (s), 1581 (s), 1536 (s), 1471 (m), 1414 (s), 1305 (m), 1258 (s), 1187 (m), 1084 (w), 1015 (w), 919 (s), 759 (s), 695 (s), 526 (w); ^{1}H-NMR (DMSO-d^6): 11.06 (1H, s, -NH), 9.05 (1H, s, Ar-H), 8.02 (2H, d, 8.4Hz, Ar-H), 7.63 (2H, d, 8.4Hz, Ar-H), 2.41 (2H, q, 7.5Hz, -CH$_2$), 1.12 (3H, t, 7.5Hz, -CH$_3$); ^{13}C-NMR (DMSO-d^6): 172.5, 169.4, 166.9, 141.1, 135.7, 131.6, 123.3, 121.2, 120.3, 31.0, 9.7. MS (ESI): m/z: 260.0 [M+Na]$^+$.

Synthesis of 2-benzamidoterephthalic acid (H$_2$L3)
This compound was synthesized by a similar pathway as that described for H$_2$L2.

In the first stage, dimethyl-2-aminoterephthalate (2.09 g, 10 mmol) and NEt_3 (1.51 g, 15 mmol) were placed in a round bottom flask and then dry dichloromethane (20 mL) was added. After cooling in an ice bath followed by dropwise addition of benzoyl chloride (1.68 g, 12 mmol) the reaction mixture was stirred overnight at room temperature. Upon removal of the solvent under reduced pressure a yellow solid was obtained. 20 mL of water were added to the yellow solid which was then extracted with dichloromethane. The organic extracts were collected over anhydrous sodium sulfate; subsequent removal of the solvent gave the methyl ester of compound H_2L3. Yield: 87% (2.72 g).

In the second step, the isolated ester (3.13 g, 10 mmol) and NaOH (0.8 g, 20 mmol) were dissolved in 20 mL of MeOH : water (4 : 1). The reaction mixture were refluxed for 4 h at 80 ˚C, after which the solvent was removed under reduced pressure, 10 mL of water were added and the solution acidified (pH=2) with dilute HCl solution. The obtained white solid product H_2L3 was filtered off and washed with water until total removal of the acid. Yield: 81% (2.31 g). Anal. Calcd. for $C_{15}H_{11}NO_5$ (M = 285.25): C, 63.16; H, 3.89; N, 4.91. Found: C, 63.11; H, 3.50; N, 4.72. FT-IR (KBr, cm^{-1}): 3140 (bs), 2582 (mb), 1694 (s), 1618 (m), 1582 (s), 1537 (s), 1465 (m), 1427 (s), 1389 (m), 1294 (s), 1248 (m), 1192 (s), 1152 (w), 1072 (w), 904 (s), 759 (s), 691 (s), 588 (w), 518(m); ^{1}H-NMR (DMSO-d^6): 12.14 (1H, s, -NH), 9.28 (1H, s, Ar-H), 8.13 (1H, d, 8.1Hz, Ar-H), 7.97 (2H, d, 6.6Hz, Ar-H), 7.59-7.75 (4H, m, Ar-H); ^{13}C-NMR (DMSO-d^6): 169.8, 166.9, 165.3, 141.3, 135.9, 134.7,132.8, 131.9, 129.5, 127.5, 123.8, 121.3, 120.7. MS (ESI): m/z: 308.0 [M+Na]$^+$.

Synthesis of [Zn$_2$(L1)$_2$(4,4'-bipyridine)$_2$(H$_2$O)(DMF)]$_n$ (1)

The mixture of $Zn(NO_3)_2.6H_2O$ (13 mg, 0.044 mmol), H_2L1 (10 mg, 0.044 mmol), and 4,4'-bipyridine (7 mg, 0.44 mmol) was dissolved in 5 mL of DMF and water (1 : 1). A white precipitate was obtained when the mixture was stirred at room temperature for 1 h. The precipitate was dissolved in 0.5 mL of 28% aqueous ammonia solution, the resulting mixture was sealed in an 8 mL glass vessel and heated at 80˚C for 48 h. Subsequent gradual cooling to room temperature (0.2 ˚C min^{-1}) afforded needle-like colorless crystals. Yield: 61% (based on Zn). Anal. Calcd. for $C_{43}H_{39}N_7O_{12}Zn_2$ (M = 976.55): C, 52.89; H, 4.03; N, 10.04; Found: C, 52.63; H, 4.00; N, 10.21. FT-IR (KBr, cm^{-1}): 3329 (bs), 1668 (s), 1610 (s), 1564 (s), 1514 (s), 1451 (w), 1422 (s), 1363 (s), 1303 (s), 1265 (m), 1245 (m), 1220 (s), 1143 (w), 1069 (s), 1046 (m), 1010 (s), 996 (m), 943 (w), 912 (m), 815 (s), 769 (s), 633 (s), 533 (w), 503 (w).

Synthesis of [Zn$_4$(L2)$_3$(OH)$_2$(DMF)$_2$(H$_2$O)$_2$]$_n$ (2)

$Zn(NO_3)_2.6H_2O$ (6.6 mg, 0.022 mmol) and H_2L2 (5 mg, 0.022 mmol) were dissolved in 4 mL of DMF: 1,4-dioxane: H_2O (2 : 1 : 1 by volume), sealed in a capped glass vessel and heated to 80˚C for 48 h. Subsequent gradual cooling to room temperature (0.2 ˚C min^{-1}) afforded colorless crystals obtained in ca. 77% yield (based on Zn). Anal. Calcd. for $C_{39}H_{46}N_5O_{21}Zn_4$ (M = 1182.29): C, 39.62; H, 3.92; N, 5.92; Found: C, 39.71; H, 4.01; N, 5.76.FT-IR (KBr, cm^{-1}) 3423 (bs), 3282 (bs), 2992 (w), 1660 (s), 1568 (s), 1514 (m), 1417 (s), 1372 (s), 1297 (w), 1255 (w), 1105 (w), 1067 (w), 921 (w), 813 (w), 775 (s), 550 (mb).

Synthesis of [Zn(L3)(H$_2$O)$_2$]$_n$. n/2(1,4-dioxane) (3)

The mixture of $Zn(NO_3)_2.6H_2O$ (26 mg, 0.088 mmol) and H_2L3 (10 mg, 0.035 mmol) was dissolved in 5 mL of DMF and 1,4-dioxane (1 : 1). A white precipitate was obtained when 0.2 mL of 28% aqueous ammonia solution was added to this reaction mixture. The precipitate was dissolved upon the addition of additional 0.5 mL of 28% aqueous ammonia solution. Then, the resulting mixture was sealed in an 8 mL

glass vessel and heated at 80 °C for 48 h. It was subsequently cooled to room temperature (0.2 °C min^{-1}), affording plate-like colorless crystals. Yield: 68% (based on Zn). Anal. Calcd. for $C_{17}H_{17}NO_8Zn$ (*M* = 428.69): C, 47.63; H, 4.00; N, 3.27. Found: C, 47.53; H, 3.92; N, 3.10. FT-IR (KBr, cm^{-1}): 3319(s), 3242(s), 3179(s), 1636(s), 1569(s), 1511(s), 1429(s), 1337(s), 1288(s), 1109(m), 1032(w), 960(w), 877(m), 819(m), 771(s), 699(s), 611(m), 558(m).

Procedure for the nitroaldol (Henry) reaction catalyzed by Zn-MOFs

In a typical reaction, a mixture of aldehyde (1 mmol), nitroethane (0.3 mL) and Zn-catalyst (29 mg for 1, 35mg of 2 and 13mg of 2, 3 mol%) was placed in a capped glass vessel then 2 mL MeOH were added into it. The mixture was heated at 70 °C for 48 h, and subsequently quenched by centrifugation and filtration at room temperature. The filtrate was evaporated in vacuum to give the crude product. The residue was dissolved in DMSO-d^6 and analyzed by ^{1}H NMR. The yield of the β-nitroalkanol product (relatively to the aldehyde) was established typically by taking into consideration the relative amounts of these compounds, as given by ^{1}H NMR and previously reported.[47] The syn/anti selectivity was calculated on the basis of ^{1}H-NMR spectra which is presented in Figure S7 (supporting information). In the ^{1}H NMR spectra, the values of vicinal coupling constants (for the β-nitroalkanol products) between the α-N–C–H and the α-O–C–H protons identify the isomers, being *J* = 7–9 or 3.2–4 Hz for the *syn* or *anti* isomers, respectively.[45]

In order to perform the recycling experiment, first we washed the used catalyst with methanol and dried at room temperature. It was then used for the nitroaldol reaction as described above.

Procedure for the transesterification reaction catalyzed by Zn-MOFs

In a typical reaction, a mixture of methyl-3-nitrobenzoate (180mg, 1 mmol) and Zn-catalyst (29 mg for 1, 35mg of 2 and 13mg of 2, 3 mol%) in 2mL EtOH was added into a capped glass vessel. The mixture was heated at 100°C for 24 h. The solution was then centrifuged to remove the catalyst. The solvent was evaporated in vacuum, leading to a crude product. The product mixture was analyzed by ^{1}H NMR in CDCl$_3$. The yield of the ethyl ester product (relatively to the methyl ester) was established typically by taking into consideration the relative amounts of these compounds, as given by ^{1}H NMR. The ^{1}H-NMR spectra is presented in Figure S8 (Supporting Information file).The centrifuged catalyst was washed several time with methanol and dried at room temperature. After that the recycling experiment was performed under the condition mentioned above.

Crystal structure determinations

X-ray quality single crystals of the compounds were immersed in cryo-oil, mounted in a nylon loop and measured 150 K (**2**) or at room temperature (**1** and **3**).Intensity data were collected using a Bruker AXS-KAPPA APEX II or a Bruker APEX-II PHOTON 100 diffractometer with graphite monochromated Mo-Kα (λ 0.71069) radiation. Data were collected using phi and omega scans of 0.5° per frame and a full sphere of data was obtained. Cell parameters were retrieved using Bruker SMART[46] software and refined using Bruker SAINT[46a] on all the observed reflections. Absorption corrections were applied using SADABS[46a]. Structures were solved by direct methods by using the SHELXS-97 package[46b] and refined with SHELXL-97[46b]. Calculations were performed using the WinGX System–Version 1.80.03[46c]. The hydrogen atoms

attached to carbon atoms and to the nitrogen atoms of **2** and **3** were inserted at geometrically calculated positions and included in the refinement using the riding-model approximation; Uiso(H) were defined as 1.2Ueq of the parent nitrogen atoms or the carbon atoms for phenyl and methylene residues and 1.5Ueq of the parent carbon atoms for the methyl groups. The hydrogen atoms of the bridging hydroxide (in **2**) and those of coordinated water molecules were located from the final difference Fourier map and the isotropic thermal parameters were set at 1.5 times the average thermal parameters of the belonging oxygen atoms; the coordinates of the H-water molecules in **1** were blocked during the refinement process. There were disordered molecules present in the structure of **2**. Since no obvious major site occupations were found for those molecules, it was not possible to model them. PLATON/SQUEEZE[46d] was used to correct the data and potential volume of 2637.7 $Å^3$ was found with 772 electrons per unit cell worth of scattering. These were removed from the model and not included in the empirical formula. The modified dataset improved the *R*1 value by *ca.* 67 %. Moreover, one of the 2-propionamidotherephalate ligands in **2** is located close to an inversion center and only three ring carbon atoms and the propionamido substituent could be located. To avoid the duplication of this substituent upon growing the fragment, the symmetry related carbon ring atoms were generated, renamed and their s.o.f. changed to 0.5 affording, as a result of this strategy, the whole molecule of ligand with occupancy of 0.5 as defined by the multiplicity of the special position. The atoms were then flanked by PART -1 and PART 0 and the structure finalized normally, though with application of geometric restraints. Least square refinements with anisotropic thermal motion parameters for all the non-hydrogen atoms and isotropic ones for the remaining atoms were employed. Crystallographic data are summarized in Table S1 (Supplementary Information file) and selected bond distances and angles are presented in Tables S3 and S4. CCDC 968209–968211for **1–3,** respectively, contain the supplementary crystallographic data for this paper. These data can be obtained free of charge from The Cambridge Crystallographic Data Centre *via* www.ccdc.cam.ac.uk/data_request/cif.

Acknowledgements

References

1. (*a*) O. M. Yaghi, M. O'Keeffe, N. W. Ockwig, H. K. Chae, M. Eddaoudi and J. Kim, *Nature*, 2003, **423**, 705-714; (*b*) L. R. MacGillivray and J. L. Atwood, *Nature*, 1997, **389**, 469-472; (*c*) B. Moulton and M. J. Zaworotko, *Chem. Rev.*, 2001, **101**, 1629-1658; (*d*) S. R. Seidel and P. J. Stang, *Acc. Chem. Res.*, 2002, **35**, 972-983; (*d*) C. Janiak and J. K. Vieth, *New J. Chem.*, 2010,**34**, 2366-2388; (e) G. Mehlana, S. A. Bourne and G. Ramon, *Dalton Trans.*, 2012, **41**, 4224-4231; (*f*) G. Mehlana, G. Ramon and S. A. Bourne, *CrystEngComm*, 2013, **15**, 9521-9529.

2. (*a*) P. J. Hagrman, D. Hagrman and J. Zubieta, *Angew. Chem., Int. Ed.*, 1999, **38**, 2638-2684; (*b*) S. R. Batten and R. Robson, *Angew.Chem., Int. Ed.*, 1998, **37**, 1460-1494; (*c*) C. Heering, I. Boldog, V. Vasylyeva, J. Sanchiz and C. Janiak, *CrystEngComm*, 2013, **15**, 9757-9768.

3. (*a*) O. R. Evans and W. Lin, *Acc. Chem. Res.*, 2002, **35**, 511-522; (*b*) W. B. Lin, Z. Y. Wang and L. Ma, *J. Am. Chem. Soc.*, 1999, **121**, 11249-11250.

4. (*a*) N. L. Rosi, J. Eckert, M. Eddaoudi, D. T. Vodak, J. Kim, M. O'Keeffe and O. M. Yaghi, *Science*, 2003, **300**, 1127-1129; (*b*) B. Kesanli, Y. Cui, M. R. Smith, E. W. Bittner, B. C. Bockrath and W. Lin, *Angew. Chem., Int. Ed.*, 2005, **44**, 72-75; (*c*) S. Kitagawa, R. Kitaura and S. Noro, *Angew.Chem., Int. Ed.*, 2004, **43**, 2334-2375.

5. (*a*) C.-D. Wu and W. Lin, *Angew. Chem., Int. Ed.*, 2007, **46**, 1075-1078; (*b*) D. N. Dybtsev, A. L. Nuzhdin, H. Chun, K. P. Bryliakov, E. P. Talsi, V. P. Fedin and K. Kim, *Angew. Chem., Int. Ed.*, 2006, **45**, 916-920; (*c*) W. Lin, *J. Solid State Chem.*, 2005, **178**, 2486-2490; (*d*) A. M. Kirillov, Y. Y. Karabach, M. V. Kirillova, M. Haukka, and A. J. L. Pombeiro, *Dalton Trans.*, 2011, **40**, 6378-6381; (*e*) M. V. Kirillova, A. M. Kirillov, M. F. C. Guedes da Silva, and A. J. L. Pombeiro, *Eur. J. Inorg. Chem.*, 2008, 3423-3427.

6. (*a*) A. J. Fletcher, E. J. Cussen, D. Bradshaw, M. J. Rosseinsky and K. M. Thomas, *J. Am. Chem. Soc.*, 2004, **126**, 9750-9759; (*b*) L. Alaerts, C. E. A. Kirschhock, M. Maes, M. A. van der Veen, V. Finsy, A. Depla, J. A. Martens, G. V. Baron, P. A. Jacobs, J. E. M. Denayer and D. E. De Vos, *Angew. Chem., Int. Ed.*, 2007, **46**, 4293-4297; (*c*) H. B. T. Jeazet, C. Staudt and C. Janiak, *Dalton Trans.*, 2012, **41**, 14003-14027; (*d*) H. – J. Holdt, S. S. Mondal, A. Bhunia, S. Demeshko, A. Kelling, U. Schilde and C. Janiak, *CrystEngComm*, 2013, **DOI:** 10.1039/C3CE42040J.

7. M. Fujita, Y. J. Kwon, S. Washizu and K. Ogura, *J. Am. Chem. Soc.*, 1994, **116**, 1151-1152.

8. (*a*) J. Y. Lee, O. K. Farha, J. Roberts, K. A. Scheidt, S. T. Nguyen and J. T. Hupp, *Chem. Soc. Rev.*, 2009, **38**, 1450-1459;(*b*) A. Dhakshinamoorthy, M. Opanasenko, J. Ćejka, and H. Garcia, *Adv. Synth. Catal.*, 2013, **355**, 247-268;(*c*) P. Valvekens, F. Vermoortele and D. D. Vos, *Catal. Sci. Technol.*, 2013, **3**, 1435-1445;(*d*) A. M. Kirillov, M. V. Kirillova, and A. J. L. Pombeiro, *Coord.Chem. Rev.*2012, **256**, 2741-2759;(*e*) A. M. Kirillov, J. A. S. Coelho, M. V. Kirillova, M. F. C. Guedes da Silva, D. S. Nesterov, K. R. Gruenwald, M. Haukka, and A. J. L. Pombeiro, *Inorg. Chem.*, 2010, **49**, 6390-6392;(*f*) Y. Y. Karabach, M. F. C. Guedes da Silva, M. N. Kopylovich, B. Gil-Hernández, J. Sanchiz, A. M. Kirillov, and A. J. L. Pombeiro, *Inorg. Chem.*, 2010, **49**, 11096-11105; (*g*) A. Karmakar, H. M. Titi, and I. Goldberg, *Cryst.Growth Des.*, 2011, **11**, 2621-2636.

9. O. K. Farha, A. M. Spokoyny, K. L. Mulfort, M. F. Hawthorne, C. A. Mirkin and J. T. Hupp, *J. Am. Chem. Soc.*, 2007, **129**, 12680-12681.

10. (*a*) M. Eddaoudi, D. B. Moler, H. Li, B. Chen, T. M. Reineke, M. O'Keeffe and O. M. Yaghi, *Acc. Chem. Res.*, 2001, **34**, 319-330; (*b*) W. Mori and S. Takamizawa, *J. Solid State Chem.*, 2000, **152**, 120-129.

11. (*a*) A. Schaate, S. Klingelhoefer, P. Behrens and M. Wiebcke, *Cryst. Growth Des.*, 2008, **8**, 3200-3205; (*b*) S. S. Kaye and J. R. Long, *J. Am. Chem. Soc.*, 2008, **130**, 806-807; (*c*) S. S. Kaye, A. Dailly, O. M. Yaghi and J. R. Long, *J. Am. Chem. Soc.*, 2007, **129**, 14176-14177.

12. (*a*) C. –B. Liu, C. –Y. Sun, L. –P. Jin, and S. –Z. Lu, *New J. Chem.*, 2004, **28**, 1019-1026;(*b*) A. L. Grzesiak, F. J. Uribe, N. W. Ockwig, O. M. Yaghi, and A. J. Matzger, *Angew. Chem., Int. Ed.*, 2006, **45**, 2553-2556; (c) K. Hirai, S. Furukawa, M. Kondo, M. Meilikhov, Y. Sakata, O. Sakata, and S.Kitagawa, *Chem.Commun.*, 2012, **48**, 6472-6474; (*d*) S. Bauer, C. Serre, T. Devic, P. Horcajada, J. Marrot, G. Ferey, and N. Stock, *Inorg.Chem.*, 2008, **47**, 7568-7576.

13. D. Sun, S. Ma, Y. Ke, D. J. Collins and H. Zhou, *J. Am. Chem. Soc.*, 2006, **128**, 3896-3897.

14. (*a*) L. Hou, J.-P. Zhang and X.-M. Chen, *Cryst. Growth Des.*, 2009, **9**, 2415-2419; (*b*) S. R. Caskey, A. G. Wong-Foy and A. J. Matzger, *Inorg. Chem.*, 2008, **47**, 7751-7756; (*c*) B. Chen, M. Eddaoudi, S. T. Hyde, M. O'Keeffe and O. M. Yaghi, *Science*, 2001, **291**, 1021-1023; (*d*) L. Hou, J.-P. Zhang, X.-M.Chen and S. Weng Ng, *Chem. Commun.*, 2008, 4019-4021.

15. D. Sun, Y. Ke, T. M. Mattox, S. Parkin and H. C. Zhou, *Inorg. Chem.*, 2006, **45**, 7566-7568.

16. Y. Liu, J. F. Eubank, A. J. Cairns, J. Eckert, V. C. Kravtsov, R. Luebke and M. Eddaoudi, *Angew. Chem., Int. Ed.*, 2007, **46**, 3278-3283.

17. X. Lin, J. Jia, X. Zhao, K. M. Thomas, A. J. Blake, G. S. Walker, N. R. Champness, P. Hubberstey and M. Schröder, *Angew. Chem., Int. Ed.*, 2006, **45**, 7358-7364.

18. X. Lin, I. Telepeni, A. J. Blake, A. Dailly, C. M. Brown, J. M. Simmons, M. Zoppi, G. S. Walker, K. M. Thomas, T. J. Mays, P. Hubberstey, N. R. Champness and M. Schröder, *J. Am. Chem. Soc.*, 2009, **131**, 2159-2171.

19. (*a*) A. Karmakar and I. Goldberg, *CrystEngComm*, 2011, **13**, 350-366; (*b*) A. Karmakar and I. Goldberg, *CrystEngComm*, 2011, **13**, 339-349.

20. (*a*) K. L. Mulfort, O. K. Farha, C. L. Stern, A. A. Sarjeant and J. T. Hupp, *J. Am. Chem. Soc.*, 2009, **131**, 3866-3868; (*b*) O. K. Farha, K. L. Mulfort and J. T. Hupp, *Inorg. Chem.*, 2008, **47**, 10223-10225.

21. (*a*) L. Ma, D. J. Mihalcik and W. Lin, *J. Am. Chem. Soc.*, 2009, **131**, 4610-4612; (*b*) Y. Cui, O. R. Evans, H. L. Ngo, P. S. White and W. Lin, *Angew. Chem., Int. Ed.*, 2002, **41**, 1159-1162.

22. (*a*) B. Chen, C. Liang, J. Yang, D. S. Contreras, Y. L. Clancy, E. B. Lobkovsky, O. M. Yaghi and S. Dai, *Angew. Chem., Int. Ed*., 2006, **45**, 1390-1393; (*b*) C.-D. Wu and W. Lin, *Angew.Chem., Int. Ed.*, 2007, **46**, 1075-1078; (*c*) S. Horike, M. Dincă, K. Tamaki and J. R. Long, *J. Am. Chem. Soc.*, 2008, **130**, 5854-5855.

23.(*a*) D. Farrusseng, S. Aguado, and C. Pinel, *Angew. Chem. Int. Ed.,* 2009, **48**, 7502–7513; (b) L. H. Wee, L. Alaerts, J. A. Martens and D. De Vos, *Metal–Organic Frameworks as Catalysts for Organic Reactions, in Metal-Organic Frameworks: Applications from Catalysis to Gas Storage* (ed D. Farrusseng), Wiley-VCH Verlag GmbH & Co. KGaA, Weinheim, Germany, 2011, 191-212.

24. (*a*) M. Shibasaki, M. Kanai, S. Matsunaga, and N. Kumagai, *Multimetallic Multifunctional Catalysts for Asymmetric Reactions: Bifunctional Molecular Catalysis* (ed. T. Ikariya, M. Shibasaki),*Topics inOrganometallic Chemistry,* Springer-Verlag Berlin Heidelberg 2011, **37**, 1-30; (*b*) F. A. Luzzio, *Tetrahedron*, 2001, **57**, 915-945. (*c*) S. E. Milner, T. S. Moody, and A. R. Maguire, *Eur. J. Org. Chem.* 2012, 3059–3067. (*d*) A. Majhi, S. T. Kadam, and S. S. Kim, *Bull. Korean Chem. Soc.* 2009, **30**, 1767-1770. (*e*) J. Boruwa, N. Gogoi, P. P. Saikia and N. C. Barua, *Tetrahedron Asym.*, 2006, **17**, 3315-3326; (*f*) S. Jammi, M. A. Ali, S. Sakthivel, L. Rout and T. Punniyamurthy, *Chem. Asian J.*, 2009, **4**, 314-320; (*g*) C. Gan, G. Lai, Z. Zhang, Z. Wang and M. Zhou, *Tetrahedron Asym.*, 2006, **17**, 725-728; (*h*) M. Shibasaki, M. Kanai and S. Matsunaga, *Aldrichim. Acta*, 2006, **39**, 31-39.

25. A. Cwik, A. Fuchs, Z. Hella and J. Clacens, *Tetrahedron*, 2005, **61**, 4015-4021.

26. (*a*) R. Ballini, G. Bosica and P. Forconi, *Tetrahedron*, 1996, **52**, 1677-1684; (*b*) G. Rosini and R. Ballini, *Synthesis*, 1988, 833-847.

27. T.Nitabaru, N.Kumagai and M. Shibasaki, *Tetrahedron Lett.*, 2008, **49**, 272-276.

28. S. Kiyooka, T. Tsutsui, H. Maeda, Y. Kanelo and K. lsobe, *Tetrahedron Lett.*, 1995, **36**, 6531-6534.

29. B.M. Choudary,M. L. Kantam and B. J. Kavita, *J.Mol. Catal. A Chem.*, 2001, **169**, 193-197.

30. R. Chinchilla, C. Najera and P. Sánchez-Agulló, *Tetrahedron Asymm.*, 1994, **5**, 1393-1402.

31. E. J. Corey and F. Y. Zhang, *Angew. Chem., Int. Ed.*, 1999, **38**, 1931-1934.

32. T. Risgaard, K. V. Gothelf and K. A. Jørgensen, *Org. Biomol. Chem.*, 2003, **1**, 153-156.

33. (*a*) T.Yamada, *Synthesis-Stuttgart*, 2004, **12**, 1947-1950; (*b*) Y. Kogami, T. Nakajima, T. Ashizawa, S. Kezuka, T. Ikeno and T. Yamada, *Chem. Lett.*, 2004, **33**, 614-615.

34. (*a*) A. Bulut, A. Aslan, and O. Dogan, *J. Org. Chem.*, 2008, **73**, 7373–7375; (*b*) M. N. Kopylovich, T. C. O. Mac Leod, K. T. Mahmudov, M. F. C. Guedes da Silva and A. J. L. Pombeiro, *Dalton Trans.*, 2011, **40**, 5352-5361; (*c*) S. F. Lu, D. M. Du, J. X. Xu, S. W. Zhang, *J. Am. Chem. Soc.*, 2006, **128**, 7418–7419; (*d*) B. M. Trost and V. S. C. Yeh, *Angew. Chem., Int. Ed.*, 2002, **41**, 861-863; (*e*) B. M. Trost, V. S. C. Yeh, H. Ito and N. Bremeyer, *Org. Lett.*, 2002, **4**, 2621-2623; (*f*) R. Kowalczyk, L. Sidorowicz, and J. Skarzewski, *Tetrahedron: Asymmetry*, 2007, **18**, 2581–2586;(*g*) Y. Kogami, T. Nakajima, T. Ikeno, and T. Yamada, *Synthesis*, 2004, 1947–1950; (*h*) D. A. Evans, D. Seidel, M. Rueping, H. W. Lam, J. T. Shaw, and C. W. Downey, *J. Am. Chem. Soc.*, 2003, **125**, 12692–12693; (*i*) M. D. Jones, C. J. Cooper, M. F. Mahon, P. R.

Raithbya, D. Apperley, J. Wolowska, and D. Collison, *J. Mol. Catal. A: Chem.*, 2010, **325**, 8–14; (*j*) M. N. Kopylovich, A. Mizar, M. F. C. Guedes da Silva, T. C. O. Mac Leod, K. T. Mahmudov, and A. J. L. Pombeiro, *Chem. Eur. J.*, 2013, **19**, 588–600; (*k*) C. Pettinari, F. Marchetti, A. Cerquetella, R. Pettinari, M. Monari, T. C. O. Mac Leod, L. M. D. R. S. Martins, and A. J. L. Pombeiro, *Organometallics*, 2011, **30**, 1616–1626; (*l*) H. Naïli, F. Hajlaoui, T. Mhiri, T. C. O. Mac Leod, M. N. Kopylovich, K. T. Mahmudov and A. J. L. Pombeiro, *Dalton Trans.*, 2013, **42**, 399–406.

35. (*a*) X.-M. Lin, T.-T.Li, Y.-W.Wang, L. Zhang, C.-Y. Su, *Chem. Asian J.*, 2012, **7**, 2796-2804; (*b*) J. –M. Gu, W. –S. Kim and S. Huh, *Dalton Trans.*, 2011, **40**, 10826-10829; (*c*) L. –X. Shi and C. –D. Wu, *Chem. Commun.,* 2011, **47**, 2928-2930.

36. (*a*) G. A. Grasa, R. M. Kissling, S. P. Nolan, *Org. Lett.*, 2002, **4**, 3583-3586. (*b*) J. Otera *Chem. Rev.*, 1993, **93**, 1449–1470; (*c*) T. J. Davison, C. Okoli, K. Wilson, A. F. Lee, A. Harvey, J. Woodford and J. Sadhukhan, *RSC Adv.*, 2013, **3**, 6226-6240; (*d*) A. Bajaj, P. Lohan, P. N. Jha, R. Mehrotra, *J. Mol. Catal. B: Enzym.* 2010, **62**, 9–14; (*e*) J. L. Moore and T. Rovis, *Carbene Catalysts*, *Topics in Current Chemistry*, 2009, **291**, 118-144.

37. (*a*) I. M. Atadashi, M. K. Aroua, A. R. Abdul Aziz, and N. M. N. Sulaiman, *J. Indus. and Eng. Chem.*, 2013, **19**, 14–26; (*b*) B. L. Salvi, and N. L. Panwarb, *Renew. and Sus. Ener.Rev.*, 2012, **16**, 3680–3689; (*c*) A. Abbaszaadeh, B. Ghobadian, M. R. Omidkhah, and G. Najafi, *Ener. Conv. and Manag.,* 2012, **63**, 138–148; (*d*) F. Motasemi and F. N. Ani, *Renew. and Sus. Ener. Rev.*, 2012, **16**, 4719–4733.

38. (*a*) D. Seebach, E. Hungerbuhler, R. Naef, D. Schnurrenberger, B. Weidmann, and M. Zuger, *Synthesis,*1982, 138-141; (*b*) R. L. E. Furlan, E. G. Mata, and O. A. Mascaretti, *Tetrahedron Lett.,* 1998, **39**, 2257-2260.

39. (*a*) H. Kwak, S. Hwa Lee, S. H. Kim, Y. M. Lee, E. Y. Lee, B. K. Park, E. Y. Kim, C. Kim, S. –J. Kim and Y. Kim, *Eur. J. Inorg. Chem.,*2008, 408-415; (*b*) J. H. Kim, J. M. Bae, H. G. Lee, N. J. Kim, K. -D. Jung, C. Kim, S. –J. Kim, and Y. Kim, *Inorg. Chem.Commun.*, 2012, **22**, 1-5; (*c*) M. Y. Hyun, I. H. Hwang, M. M. Lee, H. Kim. K. B. Kim, C. Kim, H. –Y. Kim, Y. Kim, and S. –J. Kim, *Polyhedron*, 2013, **53**, 166-171; (*d*) Y. J. Song, H. Kwak, Y. M. Lee, S. H. Kim, S. H. Lee, B. K. Park, J. Y. Jun, S. M. Yu, C. Kim, S. –J. Kim, and Y. Kim, *Polyhedron*, 2009, **28**, 1241-1252; (*e*) M. Savonnet, S. Aguado, U. Ravon, D. Bazer-Bachi, V. Lecocq, N. Bats, C. Pineland, and D. Farrusseng, *Green Chem.*, 2009, **11**, 1729-1732; (*f*) M. Pramanik, M. Nandi, H. Uyama and A. Bhaumik, *Green Chem.*, 2012, **14**, 2273-2281; (*g*) H. Kwak, S. H. Lee, S. H. Kim, Y. M. Lee, B. K. Park, E. Y. Lee, Y. J. Lee, C. Kim, S. –J. Kim, and Y. Kim, *Polyhedron,*2008, **27**, 3484-3492.

40. (*a*) K. Nakamoto, *Infrared and Raman Spectra of Inorganic and Coordination Compounds,* 5th edn, Wiley & Sons, New York, 1997; (*b*) G. Socrates, *Infrared Characteristic Group Frequencies*, Wiley, New York, 1980.

41. (*a*) K. Robinson, G. V. Gibbs, and P. H. Ribbe, *Science,* 1971, **172,** 567-570; (*b*) A. W. Addison, T. N. Rao, J. Reedijk, J. van Rijn, and G. C. Verschoor, *J. Chem. Soc. Dalton Trans.* 1984, 1349-1356; (*c*) D.

Braga, F. Grepioni, and E. Tedesco, *Organometallics*, 1998, **17**, 2669-2678; (*d*) L. Yang, D. R. Powell, and R. P. Houser *Dalton Trans.*, 2007, 955–964.

42. (*a*) M. O'Keeffe and O. M. Yaghi, *Reticular Chemistry Structure Resource*, Arizona State University, Tempe, AZ, 2005, http://rcsr.anu.edu.au/; (*b*) V. A. Blatov, *IUCr, Comput. Comm. Newslett.*, 2006, **7**, 4, http://www.topos.ssu.samara. ru/; (c) V. A. Blatov, *Struct. Chem.,* 2012*,* **23***,* 955-963.

43. V. J. Bulbule, G. K. Jnaneshwara, R. R. Deshmukh, H. B. Borate and V. H. Deshpande, *Synth. Commun.*, 2001, **31**, 3623-3626.

44. H. Kwak, S. H. Lee, S. H. Kim, Y. M. Lee, B. K. Park, Y. J. Lee, J. Y. Jun, C. Kim, S. –J. Kim, Y. Kim, *Polyhedron*, 2009, **28**, 553–561.

45. V. J. Bulbule, V. H. Deshpande, S. Velu, A. Sudalai, S. Sivasankar and V. T. Sathe, *Tetrahedron*, 1999, **55**, 9325– 9332.

46. (*a*) Bruker, *APEX2 & SAINT, AXS Inc.*, Madison, WI, 2004; (*b*) G. M. Sheldrick, *Acta Crystallogr., Sect. A: Found. Crystallogr.*, 2008, **64**, 112-122; (*c*) L. J. Farrugia, *J. Appl. Crystallogr.*, 1999, **32**, 837-838. (*d*)A. L. Spek, *Acta Crystallogr., Sect. A,* 1990, **46**, C34.

Zinc Metal Organic Frameworks: Efficient Catalysts for Diastereoselective Henry Reaction and Transesterification

Anirban Karmakar, M. Fátima C. Guedes da Silva and Armando J. L. Pombeiro*

2-acetamidoterephthalic acid, 2-propionamidoterephthalic acid and 2-benzamidoterephthalic acid are utilized to synthesize three new zinc(II) metal organic frameworks which act as heterogeneous catalysts for the diastereoselective nitroaldol (Henry) and transesterification reactions.

Zn(II) metal organic framework